

Rapid generation of high fidelity, dissipation-stabilised dimerised chain

Kian Hwee Lim  ^{1,*} Wai-Keong Mok  ^{2,†} Jia-Bin You ³ Jian Feng Kong ³ and Davit Aghamalyan  ³

¹*Centre for Quantum Technologies, National University of Singapore, 3 Science Drive 2, Singapore 117543*

²*California Institute of Technology, Pasadena, CA 91125, USA*

³*Institute of High Performance Computing, A*STAR (Agency for Science, Technology and Research), 1 Fusionopolis Way, #16-16 Connexis, Singapore 138632*

Despite the many proposals to use dissipation as a resource to prepare long-lived entangled states, the speed of such entanglement generation is usually limited by the requirement of perturbatively small driving strengths. We propose a new scheme to rapidly generate many-body entanglement between multiple spins coupled to a 1D bath stabilized by the dissipation into the bath. Our work stands in contrast to the current well known steady state protocols for entanglement generation in spins coupled to 1D baths that take a prohibitively long time, and exhibits a speedup over state-of-the-art protocols by several orders of magnitude. Importantly, the protocol works even with a local control Hamiltonian, and the timescale is independent of the system size. Our scheme can be applied to simultaneously generate a large number of spin dimer pairs, which can serve as a valuable resource for quantum metrology and teleportation-based information processing.

Introduction.— Generation of entangled quantum states plays a pivotal role in the core tasks of quantum computation [1] and quantum metrology [2]. An outstanding challenge is to generate such states with high fidelity and ensure their robustness against noise and dissipation. An elegant solution was proposed to engineer dissipation channels in order to stabilize a generated Bell state [3]. The use of dissipation as a resource, often regarded as a detriment in quantum information processing, has proven to be fruitful across a wide spectrum of physical platforms. However, despite a plethora of theoretical proposals and experimental realizations for generating entangled states with cavity quantum electrodynamics (QED) systems [3–7], ion traps [8–10], Rydberg atoms [11–14], colour centers [15–18], circuit QED [19, 20], optical lattices and spin chains [21–25], to name a few, all of them fall short in either the speed of state generation, entanglement fidelity or the aforementioned robustness to noise and dissipation. For instance, the dissipative entanglement generation schemes based on Ref. [3] rely on perturbative expansions in the system’s driving strengths, which pose fundamental limitations on the speed of entanglement generation.

At the same time, it has also been shown in [26, 27] that in chiral quantum networks where multiple locally-driven system spins are coupled to a chiral 1D bath (which could either be a waveguide or a spin chain), it is possible to also obtain many-body entangled states stabilised by the dissipation into the 1D bath. In this theoretical scheme, no perturbative expansions in the system’s driving strengths are required, and hence the speed of the protocol is not limited by the small driving strengths. An atomic implementation of this scheme on a two-species mixture of cold quantum gases has also been proposed in [21].

In this manuscript, we first demonstrate that the time-independent schemes proposed in [21, 26, 27] for generating many-body entangled states in waveguide QED and

chiral spin chains still take a prohibitively long time despite being non-perturbative in nature, leading to an inevitable tradeoff between fidelity and speed. To resolve this challenge, we propose a new protocol to generate many-body entanglement in a way that is fast, high-fidelity and robust. To the best of our knowledge, our protocol is the only one that fulfils this trifecta. We demonstrate our scheme to simultaneously generate arbitrarily many dimer pairs with high fidelity, which is several orders of magnitude faster than state-of-the-art protocols [28]. This can potentially provide a valuable resource for quantum technologies such as quantum sensors [28, 29] and teleportation-based information processing tasks.

At its core, our protocol is based on the idea that the initial state and the final entangled state are both dark states (eigenstates of the system Hamiltonian that are annihilated by the dissipators). It suffices, then, to introduce an extra time-dependent control Hamiltonian $H_{\text{extra}}(t)$ on the system to perform a qubit-like rotation in the two-dimensional decoherence-free subspace [30, 31] spanned by the initial and final states to create multi-body entanglement with high fidelity. Our scheme does not suffer from the usual drawbacks of dissipative state preparation in open systems such as the need to have time-dependent dissipators or violating the CPTP condition for open systems dynamics [32]. Furthermore, unlike in the previously proposed time independent schemes, in the case of zero chirality, we no longer require an engineered detuning pattern on the two-level systems, which saves us from further complications in terms of experimental implementation of the protocol. Remarkably, to generate dimers, the control Hamiltonian only needs to be 2-local, with non-local interactions between the dimers suppressed by destructive interference.

Our protocol has substantial advantages over the well-known transitionless quantum driving protocol (also known as counterdiabatic driving) [31–34], since we do

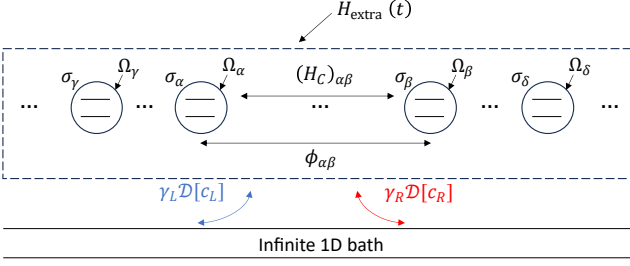


FIG. 1. Schematic for the setup, as described by Eq. (1). N spins are coupled to a waveguide as per [26] or to a 1D lattice chain with a synthetic gauge field as per [27]. Here, $\phi_{\alpha\beta}$ describe the phase picked up by the spin excitation as it travels between the α th and β th spin along the infinite 1D bath. The phase $\phi_{\alpha\beta}$ is important because it affects the bath-mediated chiral interaction between the α th and β th spin. All the spins decay collectively into the 1D bath with collective jump operators c_L and c_R and decay rates γ_L and γ_R respectively, which describe a decay into the left-going modes or the right-going modes of the 1D bath.

not require the instantaneous eigenstates of a time-dependent system Hamiltonian at all times. Counter-diabatic driving for the system considered in our paper also require chirality, while our protocol does not. We also perform a systematic study of robustness of our novel protocol to errors in the driving Hamiltonian and in the extra control Hamiltonian $H_{\text{extra}}(t)$. We also discuss the effect of chirality on our scheme and show that surprisingly, our scheme works better without chirality, in contrast to the previously proposed time-independent schemes.

Many-body entangled dark states of 1D systems. — In waveguide QED, one often considers the case where we have N spins (or 2-level systems in general) coupled to a 1D bath [27, 35]. The 1D bath serves two purposes, firstly to act as a decay channel for the system spin excitations, and secondly to mediate long-distance interactions between the system spins. With reference to Fig. 1, under the Born-Markov and rotating wave approximations, by tracing out the 1D bath, we obtain the following master equation for the N system spins (setting $\hbar = 1$) [26, 27]

$$\dot{\rho} = -i[H_S + \sum_{\alpha<\beta} (H_C)_{\alpha\beta}, \rho] + \gamma_L \mathcal{D}[c_L] \rho + \gamma_R \mathcal{D}[c_R] \rho \quad (1a)$$

$$H_S = - \sum_{\alpha=1}^N \delta_\alpha \sigma_\alpha^\dagger \sigma_\alpha + H_{\text{drive}}(t) \quad (1b)$$

$$c_L = \sum_{\alpha=1}^N e^{i\phi_\alpha} \sigma_\alpha, \quad c_R = \sum_{\alpha=1}^N e^{-i\phi_\alpha} \sigma_\alpha \quad (1c)$$

Here, σ_α is the lowering operator for the system spin indexed by α , $(H_C)_{\alpha\beta} = \frac{i}{2}(\gamma_R e^{-i\phi_{\alpha\beta}} - \gamma_L e^{i\phi_{\alpha\beta}}) \sigma_\alpha^\dagger \sigma_\beta + \text{H.c}$ describes the waveguide mediated chiral interaction be-

tween the system spins indexed by α and β , $H_{\text{drive}}(t) = \sum_{\alpha=1}^N (\Omega_\alpha(t)/2) \sigma_\alpha + \text{H.c}$ describes the local driving on the spins with Rabi frequency $\Omega_\alpha(t)$, δ_α describe the detuning between the spin indexed by α and the frequency of light in the waveguide, and $\mathcal{D}[c_{L(R)}] \rho = c_{L(R)} \rho c_{L(R)}^\dagger - \{c_{L(R)}^\dagger c_{L(R)}, \rho\}/2$ describes the leftward (rightward) dissipation of the system spins into the waveguide. The system is chiral if $\gamma_L \neq \gamma_R$, physically manifesting as an asymmetric emission into the waveguide. While entanglement generation schemes which operate in the transient were proposed [36, 37], a higher fidelity that is also robust can be attained in the steady state, using time-independent driving [26]. In particular, it was shown that subject to certain conditions on δ_α or in the chiral case $\gamma_L \neq \gamma_R$, when the spins are driven homogeneously with time-independent driving $\Omega_\alpha(t) = \Omega$, it is possible to obtain the following multipartite entangled dark steady state for even N , as a product of N_m adjacent multimers $|M_q\rangle$,

$$\rho_{ss} = |\Phi\rangle\langle\Phi|, \quad \text{where } |\Phi\rangle = \prod_{q=1}^{N_m} |M_q\rangle \quad (2a)$$

$$|M_q\rangle = a^{(0)} |g\rangle^{\otimes M_q} + \sum_{j_1 < j_2} a_{j_1, j_2}^{(1)} |S\rangle_{j_1 j_2} |g\rangle^{\otimes M_q-2} + \dots + \sum_{j_1, \dots, j_{M_q}} a_{j_1, \dots, j_{M_q}}^{(M_q/2)} |S\rangle_{j_1 j_2} \dots |S\rangle_{j_{M_q-1} j_{M_q}} \quad (2b)$$

where the summation in the last line runs over all different pairings of spins $\{(j_1, j_2), \dots, (j_{M_q-1}, j_{M_q})\}$ with $j_k < j_{k+1}$. $|S\rangle_{ij} = (|e_i\rangle|g\rangle_j - |g\rangle_j|e\rangle_i)/\sqrt{2}$ is a singlet state (or a dimer pair) between spins i and j . It can also be shown that $a^{(i)} \propto |\Omega|^{-M_q/2+i}$. In the above equation, of particular interest is the case where $N_m = 1$ which gives us $M_q = N$, since that corresponds to the most genuine entanglement (entanglement across all bipartite cuts), as well as $|\Omega| \rightarrow \infty$, since it is the most relevant for metrology [28, 29]. Hence, we shall focus on obtaining the state

$$|\Phi\rangle = \sum |S\rangle_{i_1 i_2} |S\rangle_{i_3 i_4} \dots |S\rangle_{i_{N-1} i_N} \quad (3)$$

where the summation in Eq. (3) is over different pairings of spins $\{(i_1, i_2), (i_3, i_4), \dots, (i_{N-1}, i_N)\}$ where $i_j < i_{j+1}$. By a suitable detuning pattern, it is also possible to obtain the special case where there is only one term in the sum, such that the system forms dimerised pairs of spins in the steady state. By virtue of the dissipative stabilization, the state formed is robust to perturbations and long-lived, especially at high β factors [38] where most of the system excitation is emitted into the waveguide. However, as we will show below, such schemes require a prohibitively long time to generate many-body entanglement with high fidelity.

Divergent timescale of preparing entangled dark states As mentioned in [26], for the case of $N = 2$, the timescale

required to form one dimer pair diverges as $|\Omega| \rightarrow \infty$, which is required to reach unit fidelity. This can also be shown by studying the spectral gap of the Liouvillian [39, 40] (see Appendix A). However, for the case of large N , obtaining the Liouvillian gap analytically is challenging. To this end, we use the quantum speed limit for dissipative state preparation [41] to lower-bound the timescale required to generate the state in Eq. (2) by $T_{\text{QSL}} \propto \prod_{q=1}^{N_m} |\Omega|^{M_q/2}$, which diverges as $\Omega \rightarrow \infty$. This can be interpreted as a fundamental trade-off between fidelity and speed. It is therefore imperative to propose a new scheme for rapidly generating entanglement that is similarly dissipation-stabilised.

Scheme for rapid, high fidelity many-body entanglement generation. — Our scheme deviates from the previously proposed time-independent schemes in two important aspects:

1. Instead of a time independent homogeneous drive $\Omega_\alpha = \Omega$, we consider $\Omega_j = \Omega(t)$ such that $\Omega(0) = 0$ and $\Omega(t)$ is a monotonically increasing real-valued function of t .
2. All the detunings δ_α are zero, even at zero chirality.

In this case, in the master equation Eq. (1), we have $\gamma_L \mathcal{D}[c_L] + \gamma_R \mathcal{D}[c_R] = \Gamma \mathcal{D}[c] \rho$ where $c = \sum_{\alpha=1}^N \sigma_\alpha$ and $\Gamma = \gamma_L + \gamma_R$. We also have the simplification $(H_C)_{\alpha\beta} = (i\Delta\gamma/2)(\sigma_\alpha^\dagger \sigma_\beta - \sigma_\alpha \sigma_\beta^\dagger)$ where $\Delta\gamma = \gamma_R - \gamma_L$. Since we also have $\delta_\alpha = 0$ for all spins α , the total coherent interaction terms then simplify to $H(t) \equiv H_C + H_{\text{drive}}(t)$, where $H_C = \sum_{\alpha < \beta} (H_C)_{\alpha\beta}$.

Our scheme begins by choosing a target state $|\Phi\rangle$ of the form in Eq. (3), where in the summation, we have the freedom to choose which different pairings of spins to sum over. The main idea behind our scheme comes from the fact that both the initial state $|g\rangle^{\otimes N}$ and the target state $|\Phi\rangle$ at $\Omega(t) \rightarrow \infty$ are instantaneous steady states. Then, it is clear that if we can generate the unitary $U(\theta)|g\rangle^{\otimes N} = \cos(\theta)|g\rangle^{\otimes N} - i\sin(\theta)|\Phi\rangle$ where $\theta(\Omega(t) = 0) = 0$, $\theta(\Omega(t) = \infty) = \pi/2$, then we have $U(\Omega(t) = \infty)|g\rangle^{\otimes N} = |\Phi\rangle$. One example of such a function is

$$\theta(\Omega(t)) = \frac{\pi}{2}(1 - e^{-k\Omega(t)/\Gamma}), \quad k > 0, \quad (4)$$

though many other examples exist. In practice, we do not require $\Omega(t) \rightarrow \infty$, since at $t = t_f \equiv \Omega^{-1}(\theta^{-1}(\pi/2 - \epsilon))$, the above unitary would give already us a final state $|\psi(\theta)\rangle \equiv U(\theta)|g\dots g\rangle$ that has a fidelity of $|\langle\psi(\theta)|\Phi\rangle|^2 = \cos^2(\epsilon) \approx 1 - \epsilon^2$ to $|\Phi\rangle$. Hence, by a judicious choice of $\theta(\Omega(t))$ and $\Omega(t)$, we can achieve a state $|\psi(\theta)\rangle$ that has very high fidelity to $|\Phi\rangle$ at times much shorter than the dissipation timescale Γ^{-1} . Using Eq. (4) as an example, as long as $k\Omega(t)/\Gamma \approx 4$, we would already have a state that has fidelity 0.999 to $|\Phi\rangle$. Furthermore, since $|\Phi\rangle$ is a steady state, the system stays in $|\psi(\theta)\rangle$ after applying the unitary, as long as the value of $\Omega(t)$ is fixed.

Thus, our scheme works with a high fidelity even for a finite Ω , rendering its practicality. In other words, our scheme works by finding the optimal trajectory within the decoherence-free subspace spanned by $|g\rangle^{\otimes N}$ and $|\Phi\rangle$. To construct such a unitary operator, we first define $X \equiv |g^{\otimes N}\rangle\langle\Phi| + |\Phi\rangle\langle g^{\otimes N}|$ and then immediately see that

$$U(\theta) = \exp\left(-i \int_0^t (\partial_{t'} \theta) X dt'\right) \quad (5)$$

which means that the desired $U(\theta(\Omega(t)))$ can be generated by the Hamiltonian $H_u(t) = (\partial_t \theta)X$. Thus, we simply need to add an extra time-dependent control field $H_{\text{extra}}(t) \approx H_u(t)$ to our system Hamiltonian $H(t)$. This extra time-dependent control field would only need to be switched on from $t = 0$ to $t = t_f$ for some finite t_f to generate $U(\theta)$, after which the time-dependence can be switched off and $\Omega(t)$ held constant. One might be concerned about spurious effects from the coherent waveguide-mediated interactions. While this can be entirely mitigated in $H_{\text{extra}}(t)$, we find that it is unnecessary. The validity of the approximation $H_{\text{extra}}(t) \approx H_u(t)$ is discussed in detail in Appendix C, but here we just note the following two points. Firstly, the smaller $\Delta\gamma$ is, the better this approximation is, with the best case being zero chirality ($\Delta\gamma = 0$). Secondly, defining the triplet state $|T\rangle_{ij} \equiv (|e\rangle_i|g\rangle_j + |g\rangle_i|e\rangle_j)/\sqrt{2}$, the H_{drive} term can be written as $H_{\text{drive}}(t) = H'_{\text{drive}}(t) + O(t)$ where $H'_{\text{drive}}(t) = \frac{\Omega(t)}{\sqrt{2}} \sum (|T\rangle\langle gg|_{i_1 i_2} + \dots + |T\rangle\langle gg|_{i_{N-1} i_N} + \text{H.c.})$ and $O(t) = \Omega(t) \sum (|T\rangle\langle ee|_{i_1 i_2} + \dots + |T\rangle\langle ee|_{i_{N-1} i_N} + \text{H.c.})/\sqrt{2}$, and where the sum is over all pairs $\{(i_1, i_2), (i_3, i_4), \dots, (i_{N-1}, i_N)\}$ with $i_j < i_{j+1}$. In this decomposition, $O(t)$ annihilates the decoherence-free subspace, and since it commutes with $H_u(t)$ commutes with $O(t)$, we can ignore the effect of $O(t)$. The effect of $H'_{\text{drive}}(t)$ can then also be ignored if the transformation $|g\rangle^{\otimes N} \rightarrow |\Phi\rangle$ due to $H_u(t)$ is much quicker than the transformation $|g\rangle^{\otimes N} \rightarrow |T\rangle_{i_1 i_2} \dots |T\rangle_{i_{N-1} i_N}$ due to $H'_{\text{drive}}(t)$.

It is important to highlight that by choosing $\partial_t \theta$ to be as large as possible, we can perform this transformation in this decoherence-free subspace arbitrarily quickly. Moreover, our protocol works in the non-chiral case with $\Delta\gamma = 0$, which is an improvement over [26] which requires $\Delta\gamma \neq 0$ when all the detunings δ_i are zero. Also, while this protocol looks similar to the idea of counterdiabatic driving in decoherence-free subspaces [31, 32, 34], it is different in many ways. Both schemes utilize an additional time-dependent control Hamiltonian, but unlike counterdiabatic driving, the state $|\psi(\theta)\rangle$ need not be an instantaneous eigenstate of $H(t)$. In fact, to move along the adiabatic trajectory in the Hilbert space as proposed in [26], we require $\Delta\gamma \neq 0$, whereas our scheme allows for $\Delta\gamma = 0$. This means that fundamentally, our scheme is different from the various shortcut-to-adiabaticity schemes [33]. In our computation of the

extra driving field $H_{\text{extra}}(t)$, unlike the various counter-diabatic driving schemes, we did not require all the instantaneous eigenstates of $H(t)$. This is particularly advantageous in many situations where an exact diagonalization of $H(t)$ is difficult. More details about the differences between our proposed scheme and counterdiabatic driving can be found in Appendix B.

From what is discussed above, we see that the key part is implementing the X operator, which can be experimentally difficult for certain choices of the target state $|\Phi\rangle$ due to the many-body interactions required to generate X . An example for $N = 6$ spins is shown in Appendix D. However, for the case where $|\Phi\rangle$ describes the state of $N/2$ dimerised pairs, we can apply the above formalism to arrive at $U(\theta(\Omega(t))) = U_{i_1 i_2}(\theta)U_{i_3 i_4}(\theta)\dots U_{i_{N-1} i_N}(\theta)$ where $U_{i_k i_{k+1}}(\theta) = \cos(\theta)\mathbb{1} - i\sin(\theta)X_{i_k i_{k+1}}$, and $X_{i_k i_{k+1}} = |gg\rangle\langle S|_{i_k i_{k+1}} + |S\rangle\langle gg|_{i_k i_{k+1}}$ is a two-body interaction term between spins i_k and i_{k+1} . This unitary operator $U(\theta(\Omega(t)))$ can then be generated by the Hamiltonian $H_u(t) = (\partial_t\theta)X$ where $X = X_{i_1 i_2} + X_{i_3 i_4} + \dots + X_{i_{N-1} i_N}$. In the end, we have $H_{\text{extra}}(t) \approx H_u(t)$. Thus, it suffices for the engineered control Hamiltonian to only contain up to 2-local interactions. Explicitly, for geometrically local dimer pairs, we have

$$H_{\text{extra}}(t) \approx \sum_{k \text{ odd}} V_{k, k+1} \quad (6a)$$

$$V_{k, k+1} = (\partial_t\theta) \left(\frac{1}{2}(\sigma_k^x - \sigma_{k+1}^x) + \frac{1}{2}(\sigma_k^x \sigma_{k+1}^z - \sigma_{k+1}^z \sigma_k^x) \right). \quad (6b)$$

Fig. 2 shows the results of numerical experiments comparing our scheme against previous proposals, for $N = 8$ spins forming $N/2 = 4$ geometrically local dimer pairs. We also benchmark our scheme against an adiabatic scheme that operates on the same timescales as our scheme. As can be seen, at short timescales $\Gamma t \ll 1$, our protocol achieves concurrence ≈ 1 for the case where $\Delta\gamma = 0$ and concurrence ≈ 0.91 for the case where $\Delta\gamma/\Gamma = 1$. The effect of non-zero $\Delta\gamma$ is further discussed in Appendix C. On the other hand, the adiabatic protocol fails at timescales $\Gamma t \ll 1$ as the driving strength is modulated too quickly, violating the adiabatic condition for open quantum systems [42]. This is corroborated by a sharp drop in purity between $0 < t < t_f$. After $t > t_f$ where the driving strengths become fixed, the adiabatic and the time-independent schemes become very similar. Since the control Hamiltonian is only 2-local, our scheme takes the same time for any even N and is hence scalable in generating many dimer pairs simultaneously, which is an improvement over state-of-the-art schemes [28] that require an increasingly large $\Gamma t \geq 10$ as more dimer pairs are formed.

Robustness analysis. — To investigate the robustness of our scheme, we consider two types of noise due to imperfect control. Let $\xi_1(t)$ and $\xi_2(t)$ be two independent Gaussian white noise random variables with

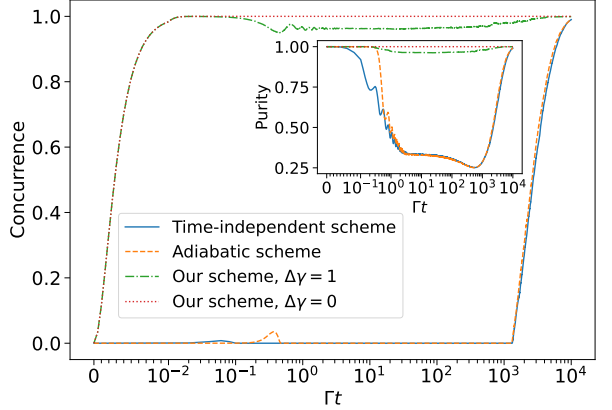


FIG. 2. In this figure we consider the case of $N = 8$ spins forming $N/2 = 4$ geometrically local dimer pairs $\{(1, 2), (3, 4), (5, 6), (7, 8)\}$. Since all dimer pairs are treated equally, we just plot the concurrence [43] and the purity (in the inset) between the spins $(1, 2)$ for various entanglement generation schemes mentioned in the paper. For our scheme, we use Eq. (4) with $k = 10$. For both our scheme and the adiabatic scheme, we use $\Omega(t)/\Gamma = m\Gamma t\Theta(t_f - t) + m\Gamma t_f\Theta(t - t_f)$ where $\Theta(t)$ is the Heaviside step function with $\Theta(0) = 1/2$, and with $m = 25$, $t_f = \Gamma^{-1}$, whereas for the time-independent scheme, we have $\Omega/\Gamma = 25$. For both the adiabatic scheme and the time-independent scheme, we have $\Delta\gamma/\Gamma = 1$, and also the appropriate detuning conditions as proposed in [26]. The adiabatic schemes and the time-independent schemes are very similar after $t > t_f$ because the driving strengths $\Omega(t)$ become fixed after $t > t_f$. Clearly, only our protocol succeeds at short timescales $\Gamma t \ll 1$.

zero mean and unit variance. A stochastic fluctuation in $H_{\text{drive}}(t)$ can be modelled by making the replacement $H_{\text{drive}}(t) \rightarrow (1 + \eta_1 \xi_1(t))H_{\text{drive}}(t)$. Similarly, a stochastic fluctuation in $H_{\text{extra}}(t)$ can be modelled by making the replacement $H_{\text{extra}}(t) \rightarrow (1 + \eta_2 \xi_2(t))H_{\text{extra}}(t)$. Following [33, 44], we average over the white noise random variables using Novikov's theorem for white noise [45] to obtain the following modified master equation

$$\dot{\rho} = -i[H_{\text{drive}}(t) + H_{\text{extra}}(t), \rho] + \Gamma \mathcal{D}[c]\rho + \eta_1^2 \mathcal{D}[H_{\text{drive}}(t)]\rho + \eta_2^2 \mathcal{D}[H_{\text{extra}}(t)]\rho \quad (7)$$

where we see that the effect of the white noise stochastic fluctuations is to add more dissipation into our state of system spins. Using $\theta(\Omega(t))$ from Eq. (4) with $k = 10$, and $\Omega(t) = mt$, $m > 0$, we numerically study the effect of η_i separately by plotting the concurrence of the dimer pair (for $N = 8$) as a function of η_i and m in Fig. 3. Our scheme is robust against noise in H_{drive} regardless of how fast $\Omega(t)$ is increased. This can be understood from the fact that our scheme works as long as $\Omega(t)/\Gamma \gg 1$ at large t , such that the fluctuations $\Omega(t)/\Gamma$ are insignificant. On the other hand, when dealing with noise in $H_{\text{extra}}(t)$, there is a tradeoff between the amount of noise

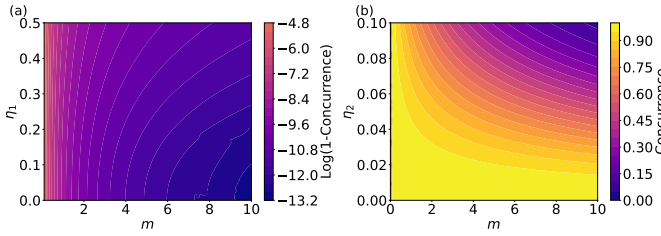


FIG. 3. Analysis of the robustness of our scheme against noise. Here, we use Eq. (4) for $\theta(\Omega(t))$ with $k = 10$ and $\Omega(t) = mt$, and we consider the case where $\Delta\gamma = 0$ in generating 4 dimerised pairs from $N = 8$ spins. Since the concurrences of all the dimers are the same, we use the concurrence of a dimer pair to characterise the entanglement generated. In (a), since the values of concurrence C of the final state obtained are all close to 1, we plot $\log(1 - C)$ against η_1 and m while assuming $\eta_2 = 0$, and in (b), we plot the concurrence of the final state obtained as a function of η_2 and m but with assuming $\eta_1 = 0$. From (a), since the values of the concurrence C are all close to 1, we see that our protocol is relatively insensitive to fluctuations in the driving strength $\Omega(t)$ regardless of how fast we increase the driving, though there is still some trade-off. From (b), we see that there is a trade-off between the amount of noise allowed and the rate m at which we can increase the driving strength Ω .

present η_2 and the maximum m allowed such that the concurrence remains high, which can be explained by the adiabatic theorem for open quantum systems [42].

Discussion. — The practicality of our scheme largely depends on the implementation of the X operator. For the case where have N spins forming $N/2$ geometrically local spin dimers, our scheme only requires 2-local control Hamiltonians which are of the form of two-body Dzyaloshinskii-Moriya (DM) interactions [46], which can be experimentally implemented in superconducting qubits via Floquet engineering [47]. Furthermore, recent experiments using superconducting qubits work with non-radiative and dephasing decay rates of $\gamma_{\text{nr}}/2\pi \approx 15$ kHz and $K_\phi/2\pi \approx 100$ kHz (corresponding to $T_1 = 1.71\mu\text{s}$ and $T_2 = 0.58\mu\text{s}$) [48]. Considering a typical decay rate of a single qubit into a waveguide $\gamma/2\pi \approx 15\text{MHz}$, from Fig. 2, it is clear that we obtain the steady state faster than the superconducting qubit decoherence times. Hence, we propose that our protocol can be implemented on superconducting qubits coupled to a 1D bath like a waveguide or a 1D lattice chain. Moreover, comparing our scheme with another state-of-the-art scheme for producing dimers that uses a squeezed vacuum [28] (which also surpasses the previously proposed time-independent schemes), we also find that our scheme has the potential to outperform this scheme by several orders of magnitude, depending on how fast $\theta(\Omega(t))$ can be experimentally modulated.

Conclusion. — We present a new scheme for rapid, high fidelity generation of multibody entanglement for spins coupled to a 1D bath such as a waveguide or a 1D

spin chain. The entanglement generated is stabilised by dissipation into the 1D bath, which means that if the β factor of the 1D bath is high, the generated entanglement will be long lived. By showing that the previously proposed time-independent schemes in [21, 26, 27] take a prohibitively long time to generate the steady state in general, we show that our scheme improves upon existing entanglement generation schemes for systems coupled to 1D baths and we believe that our scheme is the only one that is able to generate multibody entanglement for these systems in a way that is rapid, high fidelity, and robust against dissipation. Moreover, unlike the previously proposed time-independent schemes, our scheme does not require chirality and it also does not require imprinting a particular detuning pattern on the spins coupled to the 1D bath. Our scheme is also robust against noise. At its core, our scheme relies on an time-dependent extra control Hamiltonian to generate a unitary that mimics a rotation in the decoherence-free subspace spanned by the initial product state and a target entangled state, which is different from and advantageous to the so-called “shortcut to adiabaticity” schemes like counterdiabatic driving (also known as transitionless quantum driving) in decoherence free subspaces, such as in [31].

Our work opens up many avenues for research. Our scheme is able to generate many long-lived dimer pairs in a short timescale with high fidelity, and these dimer pairs can be used as resource states in teleportation-based schemes or in quantum sensors. Furthermore, following [49, 50] who proposed how the many-body interaction terms associated with counterdiabatic driving can be approximated by local driving terms, it would be interesting to see if the many-body interaction terms that arise from our scheme can be similarly approximated by local driving terms. We expect all of these to have a substantial impact of dissipation-stabilised entanglement generation in the near and far term.

The IHPC A*STAR Team acknowledges support from the National Research Foundation Singapore (Grants No. QEP-SF1), A*STAR Career Development Award (WBS No. SC23/21-8007EP), and A*STAR Delta-Q (xxx). K.H.L is grateful to the National Research Foundation and the Ministry of Education, Singapore for financial support, and to Kwek Leong Chuan for helpful discussions. WKM thank Richard Tsai and William Chen for helpful discussions.

* Equal contribution; kianhwee_lim@u.nus.edu

† Equal contribution

- [1] M. A. Nielsen and I. Chuang, Quantum computation and quantum information (2002).
- [2] V. Giovannetti, S. Lloyd, and L. Maccone, Nature photonics **5**, 222 (2011).
- [3] M. J. Kastoryano, F. Reiter, and A. S. Sørensen, Physical

- review letters **106**, 090502 (2011).
- [4] F. Reiter, M. J. Kastoryano, and A. S. Sørensen, New Journal of Physics **14**, 053022 (2012).
- [5] R. Sweke, I. Sinayskiy, and F. Petruccione, Physical Review A **87**, 042323 (2013).
- [6] S.-L. Su, X.-Q. Shao, H.-F. Wang, and S. Zhang, Physical Review A **90**, 054302 (2014).
- [7] L.-T. Shen, X.-Y. Chen, Z.-B. Yang, H.-Z. Wu, and S.-B. Zheng, Physical Review A **84**, 064302 (2011).
- [8] Y. Lin, J. Gaebler, F. Reiter, T. R. Tan, R. Bowler, A. Sørensen, D. Leibfried, and D. J. Wineland, Nature **504**, 415 (2013).
- [9] D. C. Cole, J. J. Wu, S. D. Erickson, P.-Y. Hou, A. C. Wilson, D. Leibfried, and F. Reiter, New Journal of Physics **23**, 073001 (2021).
- [10] D. C. Cole, S. D. Erickson, G. Zarantonello, K. P. Horn, P.-Y. Hou, J. J. Wu, D. H. Slichter, F. Reiter, C. P. Koch, and D. Leibfried, Physical Review Letters **128**, 080502 (2022).
- [11] R. Li, D. Yu, S.-L. Su, and J. Qian, Physical Review A **101**, 042328 (2020).
- [12] X.-Q. Shao, J.-B. You, T.-Y. Zheng, C. Oh, and S. Zhang, Physical Review A **89**, 052313 (2014).
- [13] Y.-H. Chen, Z.-C. Shi, J. Song, Y. Xia, and S.-B. Zheng, Physical Review A **97**, 032328 (2018).
- [14] D. B. Rao and K. Mølmer, Physical Review A **90**, 062319 (2014).
- [15] Y.-F. Qiao, H.-Z. Li, X.-L. Dong, J.-Q. Chen, Y. Zhou, and P.-B. Li, Physical Review A **101**, 042313 (2020).
- [16] Z. Jin, S. Su, and S. Zhang, Physical Review A **100**, 052332 (2019).
- [17] D. B. Rao, S. Yang, and J. Wrachtrup, Physical Review A **95**, 022310 (2017).
- [18] P.-B. Li, S.-Y. Gao, H.-R. Li, S.-L. Ma, and F.-L. Li, Physical Review A **85**, 042306 (2012).
- [19] Z. Leghtas, U. Vool, S. Shankar, M. Hatridge, S. M. Girvin, M. H. Devoret, and M. Mirrahimi, Physical Review A **88**, 023849 (2013).
- [20] F. Reiter, L. Tornberg, G. Johansson, and A. S. Sørensen, Physical Review A **88**, 032317 (2013).
- [21] T. Ramos, H. Pichler, A. J. Daley, and P. Zoller, Physical review letters **113**, 237203 (2014).
- [22] G. Kordas, S. Wimberger, and D. Witthaut, Europhysics Letters **100**, 30007 (2012).
- [23] T. Botzung, S. Diehl, and M. Müller, Physical Review B **104**, 184422 (2021).
- [24] G. Morigi, J. Eschner, C. Cormick, Y. Lin, D. Leibfried, and D. J. Wineland, Physical Review Letters **115**, 200502 (2015).
- [25] G. de Moraes Neto, V. Teizen, V. Montenegro, and E. Vernek, Physical Review A **96**, 062313 (2017).
- [26] H. Pichler, T. Ramos, A. J. Daley, and P. Zoller, Phys. Rev. A **91**, 042116 (2015).
- [27] T. Ramos, B. Vermersch, P. Hauke, H. Pichler, and P. Zoller, Phys. Rev. A **93**, 062104 (2016).
- [28] R. Gutiérrez-Jáuregui, A. Asenjo-Garcia, and G. S. Agarwal, Phys. Rev. Res. **5**, 013127 (2023).
- [29] P. Groszkowski, M. Koppenhöfer, H.-K. Lau, and A. A. Clerk, Phys. Rev. X **12**, 011015 (2022).
- [30] D. A. Lidar, I. L. Chuang, and K. B. Whaley, Physical Review Letters **81**, 2594 (1998).
- [31] S. L. Wu, X. L. Huang, H. Li, and X. X. Yi, Phys. Rev. A **96**, 042104 (2017).
- [32] G. Vacanti, R. Fazio, S. Montangero, G. M. Palma, M. Paternostro, and V. Vedral, New Journal of Physics **16**, 053017 (2014).
- [33] D. Guéry-Odelin, A. Ruschhaupt, A. Kiely, E. Torrontegui, S. Martínez-Garaot, and J. G. Muga, Rev. Mod. Phys. **91**, 045001 (2019).
- [34] M. V. Berry, Journal of Physics A: Mathematical and Theoretical **42**, 365303 (2009).
- [35] D. Castells-Graells, D. Malz, C. C. Rusconi, and J. I. Cirac, Phys. Rev. A **104**, 063707 (2021).
- [36] W.-K. Mok, J.-B. You, L.-C. Kwek, and D. Aghamalyan, Physical Review A **101**, 053861 (2020).
- [37] W.-K. Mok, D. Aghamalyan, J.-B. You, T. Haug, W. Zhang, C. E. Png, and L.-C. Kwek, Physical Review Research **2**, 013369 (2020).
- [38] A. S. Sheremet, M. I. Petrov, I. V. Iorsh, A. V. Poshakinskiy, and A. N. Poddubny, Rev. Mod. Phys. **95**, 015002 (2023).
- [39] V. V. Albert and L. Jiang, Phys. Rev. A **89**, 022118 (2014).
- [40] D. Manzano and P. Hurtado, Advances in Physics **67**, 1 (2018), <https://doi.org/10.1080/00018732.2018.1519981>.
- [41] J. Liu and H. Nie, Phys. Rev. A **107**, 052608 (2023).
- [42] L. C. Venuti, T. Albash, D. A. Lidar, and P. Zanardi, Phys. Rev. A **93**, 032118 (2016).
- [43] W. K. Wootters, Quantum Inf. Comput. **1**, 27 (2001).
- [44] A. Ruschhaupt, X. Chen, D. Alonso, and J. G. Muga, New Journal of Physics **14**, 093040 (2012).
- [45] E. A. Novikov, Sov. Phys. JETP **20**, 1290 (1965).
- [46] V. Mazurenko, Y. O. Kvashnin, A. Lichtenstein, and M. Katsnelson, Journal of Experimental and Theoretical Physics **132**, 506 (2021).
- [47] D.-W. Wang, C. Song, W. Feng, H. Cai, D. Xu, H. Deng, H. Li, D. Zheng, X. Zhu, H. Wang, et al., Nature Physics **15**, 382 (2019).
- [48] M. Zanner, T. Orell, C. M. Schneider, R. Albert, S. Oleschko, M. L. Juan, M. Silveri, and G. Kirchmair, Nature Physics **18**, 538 (2022).
- [49] D. Sels and A. Polkovnikov, Proceedings of the National Academy of Sciences **114**, E3909 (2017).
- [50] I. Čepaité, A. Polkovnikov, A. J. Daley, and C. W. Duncan, PRX Quantum **4**, 010312 (2023).
- [51] J. A. Gyamfi, European Journal of Physics **41**, 063002 (2020).
- [52] D. Manzano and P. Hurtado, Advances in Physics **67**, 1 (2018).
- [53] T. Kato, Journal of the Physical Society of Japan **5**, 435 (1950).

Appendix A: Liouvillian gap analysis of timescale for $N = 2$

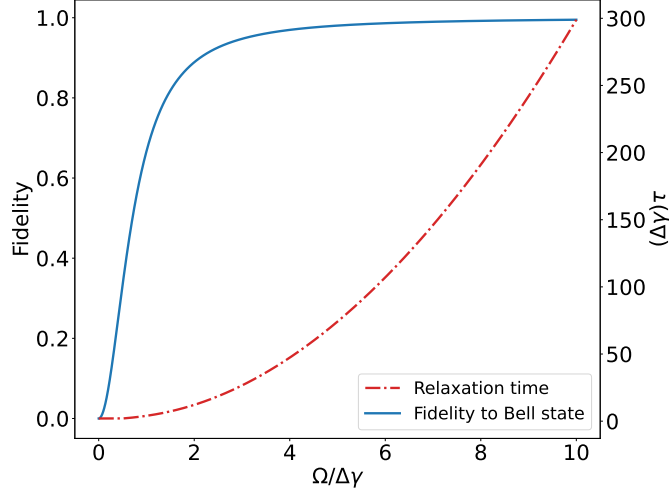


FIG. 4. Time taken to reach the steady state (left axis) and the fidelity F of the steady state to the dimer state (right axis) as a function of $\Omega/\Delta\gamma$.

Here, we perform a Liouvillian gap analysis for the case where $N = 2$ to supplement the result in the main text, which uses a different formalism [41] to prove that the timescale of forming a dimer pair diverges. Here, we assume that the phase accumulated by the excitation $\phi_{\alpha\beta}$ as it travels between two system spins is an integer multiple of 2π . Here, the two system spins are driven using a time independent Hamiltonian $H_{\text{drive}} = (\Omega/2)(\sigma_1^x + \sigma_2^x)$.

To obtain the steady state for this case, we solve Eq. (1) for $\rho_{ss} = 0$. One way to do this [51] is to vectorise the density matrix, i.e

$$\rho = \sum_{i,j} \rho_{ij} |i\rangle\langle j| \rightarrow |\rho\rangle = \frac{1}{C} \sum_{i,j} \rho_{ij} |i\rangle \otimes |j\rangle \quad (\text{A1a})$$

$$A\rho_S \rightarrow (A \otimes \mathbb{1})|\rho_S\rangle \quad (\text{A1b})$$

$$\rho_S B \rightarrow (\mathbb{1} \otimes B^T)|\rho_S\rangle \quad (\text{A1c})$$

where $|\rho\rangle$ is the vectorised form of ρ , which itself can be thought of as a ket in the so-called Liouville space [51], A and B are arbitrary operators, and B^T denotes the transpose of B . The constant C in $|\rho\rangle$ can be determined by normalising the state $|\rho\rangle$. With the above description, the master equation becomes

$$\frac{d|\rho\rangle}{dt} = L|\rho\rangle \quad (\text{A2})$$

where

$$L = -i(H \otimes \mathbb{1} - \mathbb{1} \otimes H^T) + \Gamma \left(c \otimes c^* - \frac{1}{2}(c^\dagger c \otimes \mathbb{1} - \mathbb{1} \otimes c^\dagger c) \right) \quad (\text{A3a})$$

$$H = \frac{-i\Delta\gamma}{2}(\sigma_2^\dagger\sigma_1 - \sigma_1\sigma_2^\dagger) + \frac{\Omega(t)}{2}(\sigma_1^x + \sigma_2^x) \quad (\text{A3b})$$

$$c = \sigma_1 + \sigma_2. \quad (\text{A3c})$$

Then, solving for the steady state ρ_{ss} just reduces to finding the nullspace of the matrix L . In this case, we have a unique steady state

$$\rho_{ss} = |s\rangle\langle s| \quad (\text{A4a})$$

$$|s\rangle = \frac{1}{\sqrt{2 + (\frac{\Delta\gamma}{\Omega})^2}} \left(\frac{i\Delta\gamma}{\Omega} |gg\rangle - |ge\rangle + |eg\rangle \right). \quad (\text{A4b})$$

Clearly, in the $\Omega/\Delta\gamma \rightarrow \infty$ limit, we obtain the dimer state $|S\rangle = (|ge\rangle - |eg\rangle)/\sqrt{2}$ as the steady state of our system with fidelity 1.

From L , we can also calculate the (slowest) timescale for the system to relax to the steady state by calculating the inverse of the Liouvillian gap, which is the largest non-zero real part of the eigenvalues of the matrix L [52] (note that all the non-zero eigenvalues of L have negative real parts). For $\Omega \ll \Delta\gamma$, the Liouvillian gap is $-\Delta\gamma/2$, which means that the system relaxes to the steady state at a timescale $\tau = 2/\Delta\gamma$, independent of the driving strength. On the other hand, for $\Omega \gg \Delta\gamma$, the Liouvillian gap is $-\Delta\gamma^3/(3\Omega^2)$, which means that the system relaxes to the steady state at a timescale $\tau = 3\Omega^2/\Delta\gamma^3$. In Fig. 4, we plot both the fidelity of the steady state to the dimer state as well as the timescale τ (in units of $\Delta\gamma^{-1}$) required to reach that steady state as a function of $\Omega/\Delta\gamma$. In fact, we have

$$F = \frac{2\Delta\gamma\tau}{2\Delta\gamma\tau + 3}, \quad \Delta\gamma\tau = \frac{3}{2} \left(\frac{1}{1-F} - 1 \right) \quad (\text{A5})$$

where $F = \langle S | \rho_{ss} | S \rangle$ is the fidelity of the steady state to the dimer state. This means that $\Delta\gamma\tau = \mathcal{O}((1-F)^{-1})$ as $F \rightarrow 1$. In other words, the time required to obtain a dimer state as the steady state diverges with the required fidelity of the state preparation procedure.

Appendix B: Comparison between our scheme and counterdiabatic driving

In the counterdiabatic driving scheme [32, 34], one often implements an extra time-dependent Hamiltonian $H_{\text{tqd}}(t)$ to speed up the adiabatic evolution due to a time-dependent Hamiltonian $H(t)$. Here, H_{tqd} cancels out the term in $H(t)$ that leads to transitions between different instantaneous eigenstates, and hence the system stays in its instantaneous eigenstate at all times regardless of how large $\partial_t H(t)$ is. Determining the form of $H_{\text{tqd}}(t)$ is generally a difficult process, as one needs to know all the time-dependent eigenstates of $H(t)$. Furthermore, in open quantum systems, the concept of transitionless driving is also further complicated by the need to maintain that the open systems evolution is CPTP, which might require one to engineer time-dependent dissipators [32].

However, for the problem we are considering in our paper, in the case where $\Delta\gamma \neq 0$, it is actually possible to use the idea of counterdiabatic driving in decoherence free subspaces [31]. We shall illustrate what we mean with the $N = 2$ example. From Eq. (A4), for the case where $\Delta\gamma \neq 0$, we see that by assuming $\Omega(t)$ is a monotonically increasing function of t such that $\Omega(0) = 0$, then as we slowly increase t from 0 to ∞ , we move from the instantaneous eigenstate of $H(0)$ which is $|gg\rangle$ to the instantaneous eigenstate of $H(\infty)$ which is $|S\rangle$. This follows from the adiabatic theorem of quantum mechanics [53]. Furthermore, since the instantaneous eigenstate of $H(t)$ is annihilated by c for all times t , when we use the technique of counterdiabatic driving, we avoid the complications that follow from attempting to do counterdiabatic driving for open quantum systems and we just need to consider the unitary evolution case, as mentioned in [31]. We note here that this scheme requires chirality, since if $\Delta\gamma = 0$, then there would not be an adiabatic trajectory that connects $|gg\rangle$ and $|S\rangle$.

Having explained how one might use counterdiabatic driving to speed up the many-body entanglement generation as proposed in [21, 26, 27], we note that the key difference between our scheme and counterdiabatic driving is that, for all intermediate times t between $t = 0$ and $t \rightarrow \infty$, there is no need for our system state to be an instantaneous eigenstate of $H(t)$. This is reflected in how our scheme allows for arbitrary choices of the function $\theta(\Omega(t))$ that fulfil $\theta(\Omega(0)) = 0$ and $\theta(\Omega(t \rightarrow \infty)) = \pi/2$. One practical implication of that is that unlike counterdiabatic driving, we do not require chirality. Furthermore, since counterdiabatic driving prevents transitions between all instantaneous eigenstates of $H(t)$, the construction of H_{tqd} would require knowledge of all of the eigenstates of $H(t)$ for all times t . On the other hand, since our scheme is only interested in constructing a trajectory between $|g \dots g\rangle$ and $|S\rangle_{i_1 i_2} |S\rangle_{i_3 i_4} \dots |S\rangle_{i_{N-1} i_N}$, we do not need to know all of the instantaneous eigenstates of $H(t)$.

To give a concrete example, we perform a comparison between our scheme and the counterdiabatic scheme for the $N = 2$ case. For the counterdiabatic driving scheme, we use $\gamma_R = 1, \gamma_L = 0$ which gives us $\Delta\gamma = 1$ and $\Gamma = 1$, whereas for our scheme, we use $\gamma_R = 0.5, \gamma_L = 0.5$ which gives us $\Delta\gamma = 0$ and $\Gamma = 1$. For our scheme, we also use Eq. (4) with $k = 10$ for $\theta(\Omega(t))$. In both cases, we use $\Omega(t) = mt$ with the same value of m , and after $\Gamma t = 1$, we switch off the extra control field and we stop increasing the driving strength. For this case, we have:

$$H_{\text{tqd}}(t) = \frac{1}{2} \frac{m}{1 + 2m^2t^2} (\sigma_1^x - \sigma_2^x + \sigma_1^x \sigma_2^z - \sigma_1^z \sigma_2^x) + \frac{1}{2} \frac{2m^2t}{1 + 6m^2t^2 + 8m^4t^4} (\sigma_1^x \sigma_2^y + \sigma_1^y \sigma_2^x) + \frac{1}{2} \frac{m}{1 + 6m^2t^2 + 8m^4t^4} (-\sigma_1^x + \sigma_2^x + \sigma_1^x \sigma_2^z - \sigma_1^z \sigma_2^x) \quad (\text{B1a})$$

whereas for our scheme, we have $H_{\text{extra}}(t)$ as given in Eq. (6a). Notice that $H_{\text{extra}}(t)$ is simpler than $H_{\text{tqd}}(t)$ to implement experimentally as it has lesser many-body interaction terms. The simulation results are given in Fig. 5.

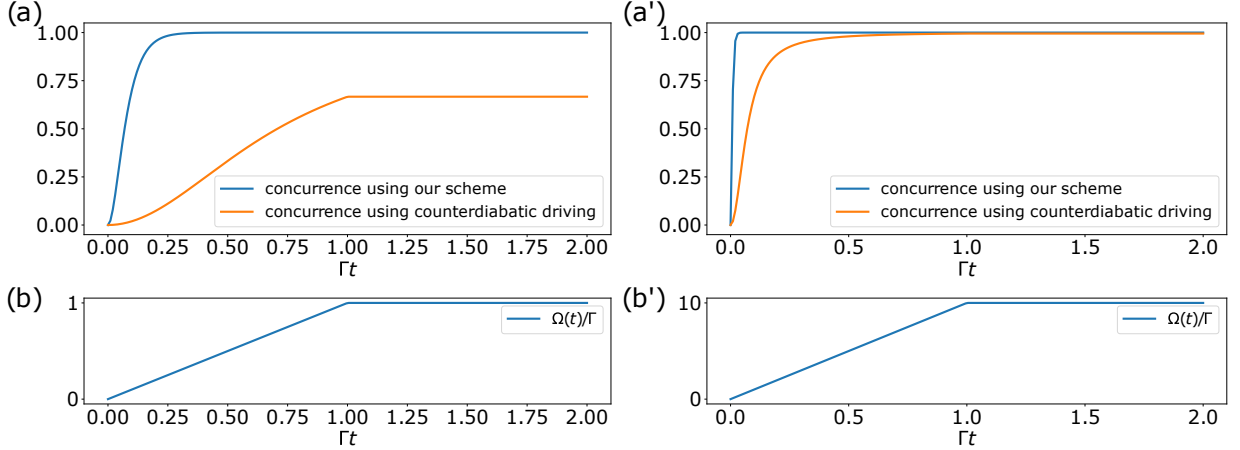


FIG. 5. In (a) and (a'), for the $N = 2$ case, we plot the concurrence of our scheme and the counterdiabatic driving scheme for $m = 1$ and $m = 10$ respectively, and in (b) and (b'), we show the time variation of the driving strengths $\Omega(t)$ against time. For our scheme, we use Eq. (4) with $k = 10$ for $\theta(\Omega(t))$. Clearly, our scheme outperforms the counterdiabatic driving scheme, since we do not need to stay in the instantaneous eigenstate of $H(t)$ given in Eq. (A4).

Notice that after $t = 1$, since the counterdiabatic driving case requires us to stay in the instantaneous eigenstate of $H(t)$ given by Eq. (A4), the largest concurrence we can get is

$$C = \frac{2m^2t^2}{1 + 2m^2t^2} \quad (\text{B2})$$

which is the fidelity of Eq. (A4) to the dimer state $|S\rangle$. Hence as can be seen from Fig. 5, for the case where $m = 1$, we have a maximal concurrence of $2/3$ only. On the other hand, for our scheme, we can very quickly get concurrence 1 since we do not need to follow the adiabatic trajectory to get the final state $|S\rangle$.

Appendix C: Approximation of H_{extra}

In writing $H_{\text{extra}}(t) = H_u(t)$ in the main text, we made two approximations, first by ignoring $-H_C$ and next by ignoring $-H'_d(t)$ in $H_{\text{extra}}(t)$. Here, we study the effect of both approximations. Here, we consider the problem of obtaining the state Eq. (3) for general even N .

Effect of ignoring $-H_C$

Clearly, when $\Delta\gamma = 0$, ignoring $-H_C$ has no effect since $H_C = 0$. Hence, here we consider the case where $\Delta\gamma \neq 0$. For general even N , the steady state of Eq. (1) is Eq. (2), where as mentioned above, we consider the case where we have only one multimer, i.e $N_m = 1$. For $|M_q\rangle$ in Eq. (2), we can show that the coefficient in front of the $|g\dots g\rangle \propto \Delta\gamma^{N/2}$.

Now, our scheme consists of switching on $H_{\text{extra}}(t)$ from $t = 0$ to $t = t_f$ where $t_f \equiv \Omega^{-1}(\theta^{-1}(\pi/2 - \epsilon))$ is as defined in the main text. After $t = t_f$, we switch off the extra driving field and keep the driving strength $\Omega(t)$ at a constant finite value $\Omega(t_f)$. As mentioned in the main text, this will give us a final state $|f\rangle$ that is $1 - \epsilon^2$ away in fidelity from Eq. (3). At this point, since $\Delta\gamma \neq 0$ and since $\Omega(t)$ is finite, the state $|f\rangle$ is not an instantaneous eigenstate of $H(t)$. Hence, there will be transitions induced by $H(t)$ on $|f\rangle$ to all the instantaneous eigenstates of $H(t)$, some of which are not dark states. Hence, the state becomes mixed and the fidelity to Eq. (3) drops. Note that depending on the choice of $\theta(t)$, since $|H_{\text{extra}}(t)| \propto \partial_t\theta$, if $\partial_t\theta \approx 0$ before t_f , then the above effect becomes more pronounced since we obtain the final state $|f\rangle$ before t_f . However, if $\Delta\gamma/\Omega(t)$ is small enough, then the probability amplitude of $|g\dots g\rangle$ component in the dark state given in Eq. (2) will be small, which means that the overlap between the $|f\rangle$ and the

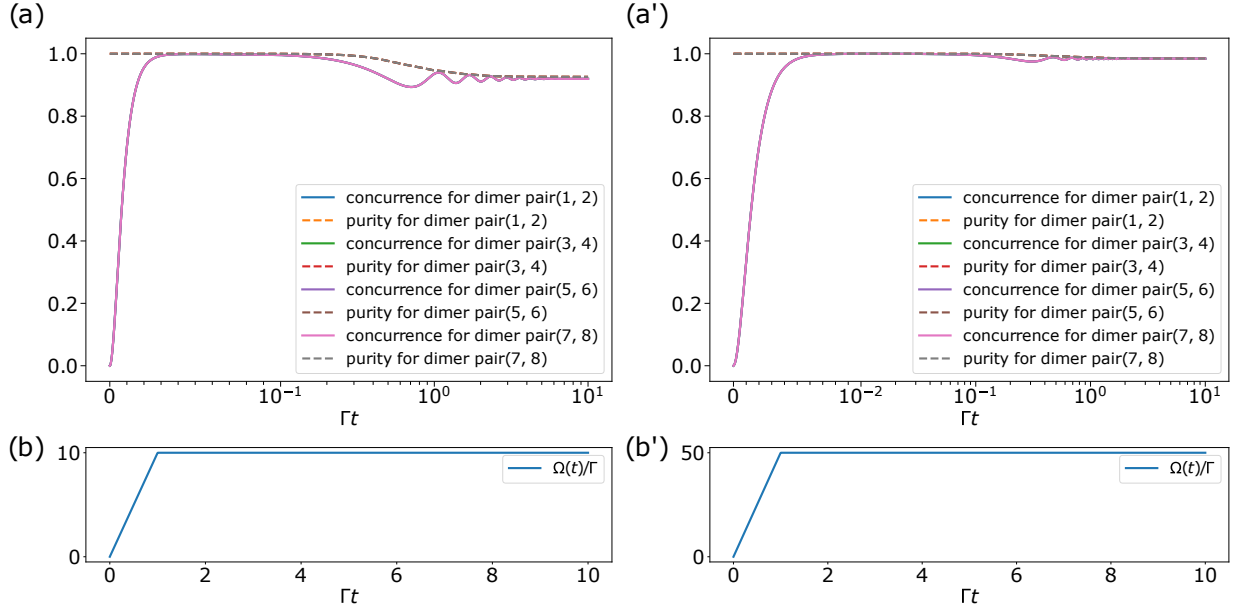


FIG. 6. Here, we study the effect of ignoring $-H_C$ in H_{extra} when $\Delta\gamma \neq 0$. In (a) and (a'), for the case where we have $N = 8$ spins forming 4 dimers, we plot both the concurrences of the dimer pairs as well as the purity of the dimer pairs for $m = 10$ and $m = 50$ respectively. In (b) and (b'), we plot the variation of the driving strength $\Omega(t)$ as a function of time. As can be seen, in both (a) and (a'), we quickly obtain the state $|\Phi\rangle$, even before we switch off $H_{\text{extra}}(t)$. This is because the form of Eq. (4) with $k = 10$ causes $H_{\text{extra}}(t)$ to be very close to zero even before $\Gamma t = 1$. Then, in (a), since Ω is not high enough, the state $H(t)$ induces transitions on $|\Phi\rangle$ and together with the jump operators, we get a mixed state. In (a'), since Ω is high enough, the transitions induced by $H(t)$ are largely onto the dark state and hence the state largely remains pure.

dark state will be large. This means that the transitions induced by $H(t)$ on $|f\rangle$ will largely be to the dark state, which means that the fidelity to Eq. (3) remains high.

We illustrate the above with the $N = 8$ case where we form 4 dimers, i.e where our target steady state is $|\Phi\rangle = |S\rangle_{12}|S\rangle_{34}|S\rangle_{56}|S\rangle_{78}$. For our scheme, we use $\gamma_R = 1, \gamma_L = 0$ which gives us $\Delta\gamma = 1$ and $\Gamma = 1$. Here, we consider $\Omega(t) = mt, m > 0$, and after $t = t_f = 1/\Gamma$, we switch off $H_{\text{extra}}(t)$ and fix $\Omega(t)$ at the constant value $\Omega(t_f)$. We also choose $\theta(\Omega(t))$ according to Eq. (4) with $k = 10$. In Fig. 6 we show the extent of the negative effect that chirality has on our system at different values of $\Omega(t_f)$.

Effect of ignoring $-H'_{\text{drive}}(t)$

As mentioned in the main text, we can ignore $-H'_{\text{drive}}(t)$ if the transformation $|g \dots g\rangle \rightarrow |\Phi\rangle$ due to $H_u(t)$ is much quicker than the transformation $|g \dots g\rangle \rightarrow |T\rangle_{i_1 i_2} \dots |T\rangle_{i_{N-1} i_N}$ due to $H'_{\text{drive}}(t)$. This can be done in many ways, for example by choosing $\theta(\Omega(t))$ according to Eq. (4) with a large value of k . An example for the $N = 8$ case where we form 4 dimers, i.e where our target steady state is $|\Phi\rangle = |S\rangle_{12}|S\rangle_{34}|S\rangle_{56}|S\rangle_{78}$ is shown in Fig. 7 below. Since we studied the effect of a non-zero $\Delta\gamma$ above, here we set $\Delta\gamma = 0$ to solely study the effect of ignoring $H'_{\text{drive}}(t)$. As can be seen from Fig. 7, for small k such that the transformation $|g \dots g\rangle \rightarrow |\Phi\rangle$ is slow, the effect of ignoring $H'_{\text{drive}}(t)$ leads to quite substantial errors, but for large k , we can safely ignore $-H'_{\text{drive}}(t)$.

Appendix D: $N = 6$ multimers

First, we show numerically that our scheme works for a $N = 6$ multimer, i.e when our target state is

$$|\Phi\rangle = \sum |S\rangle_{i_1, i_2} |S\rangle_{i_3, i_4} |S\rangle_{i_5, i_6} \quad (\text{D1})$$

where the summation is over all possible pairs $\{(i_1, i_2), (i_3, i_4), (i_5, i_6)\}$ where $i_k < i_{k+1}$. By counting, we see that for N spins, we would have $(N-1)(N-3)\dots 1$ terms in the summation. Hence, for $N = 6$, this gives us 15 terms in our

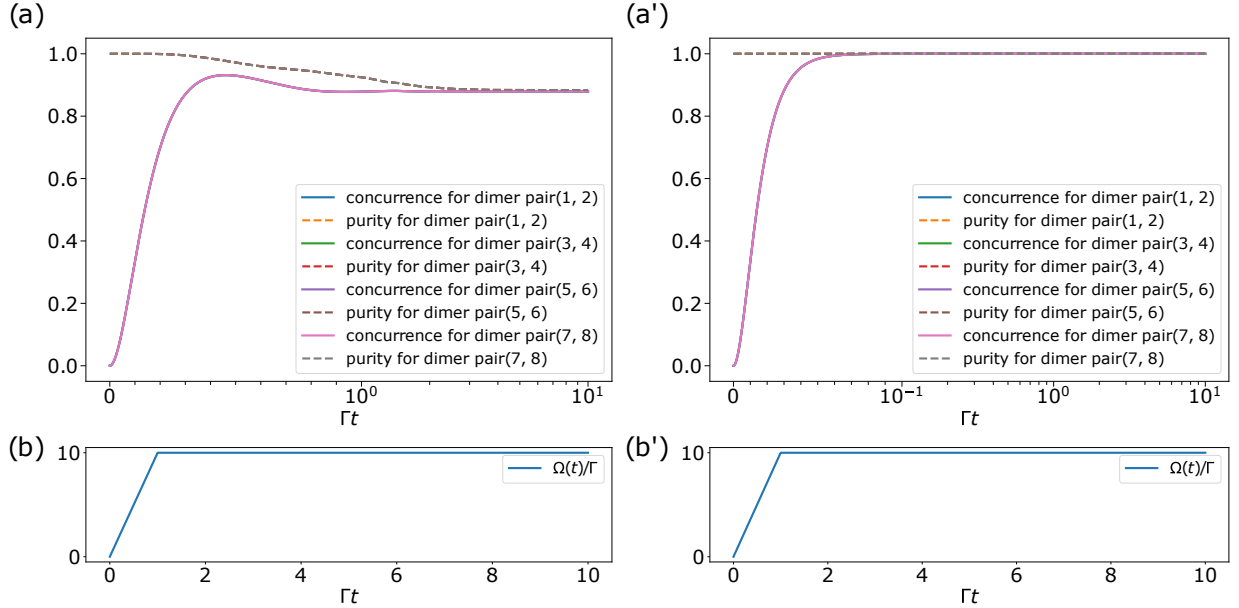


FIG. 7. Here, we study the effect of ignoring $-H'_{\text{drive}}$ in H_{extra} when $\Delta\gamma = 0$. In (a) and (a'), for the case where we have $N = 8$ spins forming 4 dimers, we plot both the concurrences of the dimer pairs as well as the purity of the dimer pairs for $m = 10$. In (b) and (b'), we plot the time variation of the driving strength $\Omega(t)$. In both (a) and (a'), we use Eq. (4) for $\theta(\Omega(t))$ with $k = 0.5$ and $k = 5$ respectively. Clearly, it is permissible to ignore $-H'_{\text{drive}}$ at large k . This is because the system goes from $|g\dots g\rangle$ so rapidly that $-H'_{\text{drive}}$ has no effect.

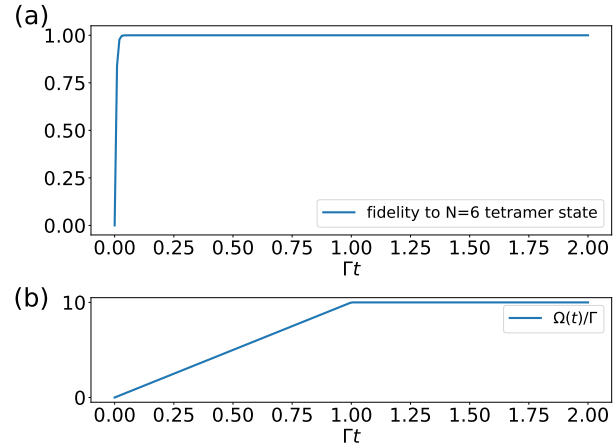


FIG. 8. In (a), we plot the fidelity of the system state to $|\Phi\rangle$, and in (b), we plot the time variation of the driving strength $\Omega(t)$. The numerical results here show that at least in theory, our scheme works.

summation. Using $\Omega(t) = mt$, $m > 0$ and Eq. (4) for $\theta(\Omega(t))$, in the case where $\Delta\gamma = 0$, a straightforward application of our scheme gives us the results in Fig. 8. Clearly, we are able to easily obtain the state $|\Phi\rangle$ numerically, and we are able to do so in $\Gamma t \ll 1$. However, for this case, the X operator is a linear combination of multiple many-body interaction terms, which means that experimental implementation of this protocol is still quite tricky with the current state of quantum control.